Available online at www.sciencedirect.com
ScienceDirect
International Journal of Machine Tools & Manufacture 48 (2008) 733–745
INTERNATIONAL JOURNAL OF MACHINE TOOLS & MANUFACTURE DESIGN, RESEARCH AND APPLICATION
www.elsevier.com/locate/ijmactool

Feed optimization for five-axis CNC machine tools with drive constraints

B. Sencer, Y. Altintas*, E. Croft

Manufacturing Automation Laboratory, The University of British Columbia, Vancouver, BC, Canada

Received 9 July 2007; received in revised form 21 December 2007; accepted 1 January 2008
Available online 18 January 2008

Abstract

Real time control of five-axis machine tools requires smooth generation of feed, acceleration and jerk in CNC systems without violating the physical limits of the drives. This paper presents a feed scheduling algorithm for CNC systems to minimize the machining time for five-axis contour machining of sculptured surfaces. The variation of the feed along the five-axis tool-path is expressed in a cubic B-spline form. The velocity, acceleration and jerk limits of the five axes are considered in finding the most optimal feed along the tool-path in order to ensure smooth and linear operation of the servo drives with minimal tracking error. The time optimal feed motion is obtained by iteratively modulating the feed control points of the B-spline to maximize the feed along the tool-path without violating the programmed feed and the drives' physical limits. Long tool-paths are handled efficiently by applying a moving window technique. The improvement in the productivity and linear operation of the five drives is demonstrated with five-axis simulations and experiments on a CNC machine tool.

Keywords: CNC; Five axis; Feed optimization

1. Introduction

Five-axis machine tools are widely used in machining parts with complex sculptured surfaces such as dies, molds and impellers. The goal of the industry is to maximize the material removal rate without violating the tolerance of the part while avoiding damage on the machine tool and cutter. The process is affected by machine tool vibrations, the machinability of the material and the accuracy of the CNC system. This paper proposes an optimal feed scheduling along a five-axis tool-path without violating the limits of the drives, which leads to more accurate CNC performance and reduced machining time.

Five-axis NC tool-paths are generated by CAD/CAM systems as cubic or NURB splines, which can be processed by modern CNC systems. Although a constant feed is programmed in the NC block, the velocity, acceleration and jerk on all five drives may continuously vary as a function of path curvature and inverse kinematics of the machine tool. If the velocity, acceleration and jerk of each drive exceed its physical saturation limits, the linear operation of the servo control is violated leading to severe marks on the surface or instability of the controller. In the current practice, conservative constant feed speeds are selected for sections of the tool-path or sometimes a single speed for the whole path so that the axis limits are never violated, which may lead to lengthy machining times, since the programmed feed is never reached by the machine tool. This paper presents optimal scheduling of the feed along the splined path while respecting the machine tool drive limits.

The identification of optimal feed profile without exceeding the saturation limits of the actuators is a nontrivial optimization problem, and studied mainly by the robotics researchers. Bobrow et al. [1] and Shin and McKay [2] were the first to solve the minimum time control

*Corresponding author. Tel.: +1 604 8225 622.
E-mail address: altintas@mech.ubc.ca (Y. Altintas).
URL: http://www.mech.ubc.ca/~mal. (Y. Altintas).

0890-6955/$ - see front matter © 2008 Elsevier Ltd. All rights reserved.
doi:10.1016/j.ijmachtools.2008.01.002

Nomenclature

x, y, z, a, c five-axis CNC machine tool axis coordinates

s path displacement along the spline tool-path

$\dot{s}(s), \ddot{s}(s), \dddot{s}(s)$ tangential velocity (feed), acceleration and jerk profiles as a function of the path displacement along the path

S_i length of each spline segment

f_i feed at B-spline control points

$N_{i,3}$ cubic basis (interpolation) functions of the B-spline

$P = [P_x \quad P_y \quad P_z]$ tool tip position vector and its scalar components (mm)

$O = [O_x \quad O_y \quad O_z]$ orientation vector and its scalar components

$R(s) = [P\{P_x(s), P_y(s), P_z(s)\}, O\{O_x(s), O_y(s), O_z(s)\}]^{\mathrm{T}}$ the pose vector of the tool defined in the workpiece coordinates

$\mathbf{q}_{5\times1}(s) = [x(s), y(s), z(s), a(s), c(s)]^{\mathrm{T}}$ axis position interpolation vector function and its five scalar components

$\dot{\mathbf{q}}_{5\times1}, \ddot{\mathbf{q}}_{5\times1}, \dddot{\mathbf{q}}_{5\times1}$ vectors containing the axis velocity, acceleration and jerk profiles, respectively

$\mathbf{q}_s = [x_s(s), y_s(s), z_s(s), a_s(s), c_s(s)]^{\mathrm{T}}$,
$\mathbf{q}_{ss} = [x_{ss}(s), y_{ss}(s), z_{ss}(s), a_{ss}(s), c_{ss}(s)]^{\mathrm{T}}$,
$\mathbf{q}_{sss} = [x_{sss}(s), y_{sss}(s), z_{sss}(s), a_{sss}(s), c_{sss}(s)]^{\mathrm{T}}$ vectors containing the first, second and third derivatives of the five axes positions with respect to the path displacement (s), respectively

$\mathbf{q}_s^v(s) = [q_{s,1}^v(s), q_{s,2}^v(s), \ldots, q_{s,5}^v(s)]^{\mathrm{T}}$ vector containing the velocity limit normalized first derivatives of the axis positions

$\mathbf{q}_s^a(s) = [q_{s,1}^a(s), q_{s,2}^a(s), \ldots, q_{s,5}^a(s)]^{\mathrm{T}}$,
$\mathbf{q}_{ss}^a(s) = [q_{ss,1}^a(s), q_{ss,2}^a(s), \ldots, q_{ss,5}^a(s)]^{\mathrm{T}}$ vectors containing the acceleration limit normalized first and second derivatives of the axis positions

$\mathbf{q}_s^j(s) = [q_{s,1}^j(s), q_{s,2}^j(s), \ldots, q_{s,5}^j(s)]^{\mathrm{T}}$,
$\mathbf{q}_{ss}^j(s) = [q_{ss,1}^j(s), q_{ss,2}^j(s), \ldots, q_{ss,5}^j(s)]^{\mathrm{T}}$,
$\mathbf{q}_{sss}^j(s) = [q_{sss,1}^j(s), q_{sss,2}^j(s), \ldots, q_{sss,5}^j(s)]^{\mathrm{T}}$ vectors containing the jerk limit normalized first, second and third derivatives of the axis positions

$\mathbf{C}_{5\times1}(s)$ optimization constraint vector function

$\dot{s}_{V,\max}(s)$, $\dot{s}_{A,\max}(s)$, $\dot{s}_{J,\max}(s)$ maximum path velocities with respect to axis velocity, acceleration and jerk limits, respectively

problem. They considered the trajectory generation as a dynamic system with two states, e.g. path displacement (s) and velocity ($\dot{s}$), and proved that the actuator torque constraints limit the velocity along the tool-path. They switched the acceleration ($\ddot{s}$) between its maximum and minimum limits at the identified path points to generate a bang-bang style trajectory. Shiller and Lu [3,4] developed reliable search procedures to find the switching points. Other methods, such as dynamic programming (DP) [5] or Pontryagin's minimum principle [6] have also been applied to solve the optimal control problem more efficiently. The machine tool literature has implemented some of those approaches in the cartesian machining of spline tool-paths. Smith et al. [7] used the acceleration limits to generate the velocity limiting curve, and implemented a similar approach to Shiller and Lu to find the optimal feed-rate profile along spline tool-paths for two-axis cartesian case. Renton and Elbestawi [8] outlined a computationally efficient two-pass algorithm to solve the minimum time feed optimization problem. The algorithm works by scanning through the trajectory in the forward and reverse directions. Dong and Stori [9] have also included a series of machine tool capability constraints, and presented a two-pass structure. Unfortunately, such trajectories possess discontinuous acceleration and torque profiles, defeating the essential purpose of using a smooth tool-path and leading to inaccurate contouring in high speed machining.

In the interest of smoothing the trajectory and enhancing the tracking performance, the jerk limits of the drives have been considered as constraints at the expense of increased computational complexity, requiring iterative solutions as opposed to optimal control formulations [10]. Piazzi and Visioli [11] used axis jerk; Constantinescu and Croft [12] used the torque rate constraints, and iteratively optimized the spline trajectories for minimum time motion of robotic manipulators. Jerk limited trajectories have also been adapted for machine tools, and computationally efficient methods have always been favored for implementation on real time CNCs. A practical feed modulation solution was proposed by Weck et al. [13] for multi-axis machine tools following quintic spline tool-paths. They considered velocity and acceleration limits of the machine tool axis to determine a conservative feed for each spline segment of the tool-path. The discrete feeds are connected with jerk limited cubic acceleration trajectory profile without considering the jerk limits of the drives. Altintas and Erkorkmaz [14] later defined the displacement profile as a minimum jerk quintic spline of time along the tool-path, and optimized the travel time of each segment iteratively. They considered velocity, acceleration, and the jerk limits of the drives for a smoother motion. Although, their approach is extendible for any type of multi-axis machine tool, the number of constraints to be considered increases dramatically with the number of axis. For instance, 14 constraints are used in the two-axis

case, which must be increased to 32 for the five-axis machines.

A computationally efficient feed scheduling algorithm is presented here for five-axis machining operations. The feed along the tool-path is optimized in a computationally efficient manner by respecting the velocity, acceleration and jerk limits of all five drives. The identified feeds at the discrete path points are fit to a cubic spline to ensure smooth trajectory along the tool-path. The algorithm is demonstrated with simulations and experiments on five-axis flank milling of an impeller blade.

2. Minimum time feed optimization problem

The objective of the paper is to minimize five-axis machining time while respecting both process and machine tool constraints. The process constraint is the vector feed along the tool-path, which is defined in the NC program by the process planner. The machine tool constraints are the velocity, acceleration/torque, and jerk limits of all active linear and rotary feed drives. As illustrated in Fig. 1, the feed ($\dot{s} = \mathrm{d}s/\mathrm{d}t$) must be scheduled along the tool-path (s) in such a way that the constraints are not violated. As a consequence, the acceleration ($\ddot{s} = \mathrm{d}^2s/\mathrm{d}t^2$) and jerk ($\dddot{s} = \mathrm{d}^3s/\mathrm{d}t^3$) along the tool-path also become path dependent as follows:

$$\left.\begin{aligned} \dot{s} &= \dot{s}(s) \\ \ddot{s}(s) &= \frac{\mathrm{d}\dot{s}(s)}{\mathrm{d}s}\frac{\mathrm{d}s}{\mathrm{d}t} = \frac{\mathrm{d}\dot{s}(s)}{\mathrm{d}s}\dot{s}(s) \\ \dddot{s}(s) &= \frac{\mathrm{d}\ddot{s}(s)}{\mathrm{d}s}\frac{\mathrm{d}s}{\mathrm{d}t} = \frac{\mathrm{d}^2\dot{s}(s)}{\mathrm{d}s^2}\dot{s}^2(s) + \left(\frac{\mathrm{d}\dot{s}(s)}{\mathrm{d}s}\right)^2\dot{s}(s) \end{aligned}\right\}. \tag{1}$$

Let us consider an arbitrary splined path (S) passing through knots P_k with a total length of $S_\Sigma = \sum_{k=1}^{N_p-1} S_k$ (see Fig. 2). The instantaneous feed along the path is $\dot{s} = \mathrm{d}s/\mathrm{d}t$; equivalently, the differential time ($\mathrm{d}t$) to travel along infinitesimal path segment ($\mathrm{d}s$) is $\mathrm{d}t = \mathrm{d}s/\dot{s}$. The feed optimization problem is defined as the minimization of total travel time (T_Σ) along the entire path (S_Σ), while respecting a set of physical limits (**C**) of the machine and process.

$$\begin{aligned} \min(T_\Sigma) = \min_{\dot{s}} \int_0^{S_\Sigma} \frac{\mathrm{d}s}{\dot{s}(s)} \quad &\text{subject to } \{\dot{s}, \ddot{s}, \dddot{s}\} \\ \leqslant C\{\text{Axis Limits}\} \quad &\text{for } 0 \leqslant s \leqslant S_\Sigma. \end{aligned} \tag{2}$$

The tangential feed ($\dot{s}$), acceleration ($\ddot{s}$) and jerk ($\dddot{s}$) are typically fitted as functions of time (t) to cubic or quintic splines in order to avoid discontinuities in the multi-axis trajectory [13,14]. An arc length parameterized cubic B-spline is used to define the feed profile as a function of path position in this paper.

$$\begin{aligned} \dot{s}(s) &= N_{0,3}(s)f_0 + N_{1,3}(s)f_1 + \cdots + N_{n-1,3}(s)f_{n-1} \\ &= \sum_{i=0}^{n-1} N_{i,3}(s)f_i, \end{aligned} \tag{3}$$

where $N_{i,3}(s)$ are the basis functions of the B-spline, and f_i ($i = 0, 1, \ldots, n-1$) are the n control points used as optimization variables in modulating the feed profile along the tool-path. The details of evaluating the B-spline adapted to feed optimization algorithm is given in the appendix.

The feed affects the chip load, hence the cutting force. The tangential acceleration along the path may be limited to dampen the aggressive motions along the path, and tangential jerk may be constrained to avoid exciting path dependent structural modes of the machine tool. However, the physical limits are the velocity, acceleration and jerk capacities of individual drives on the machine which should not be violated in order to avoid actuator saturation during five-axis contour machining. A typical five-axis motion command in workpiece coordinate system is given by a sequence of discrete positions of the cutter along the path. Each tool position is defined by three cartesian coordinates of its center $P = [P_x \quad P_y \quad P_z]$ and angular orientation vector of the cutter axis $O = [O_x \quad O_y \quad O_z], |\vec{O}| = 1$ as

$$R = [P, O]^{\mathrm{T}}. \tag{4}$$

The sequence of N_p tool positions are fitted to a cubic, quintic, Nurb or B-Splines in order to interpolate the

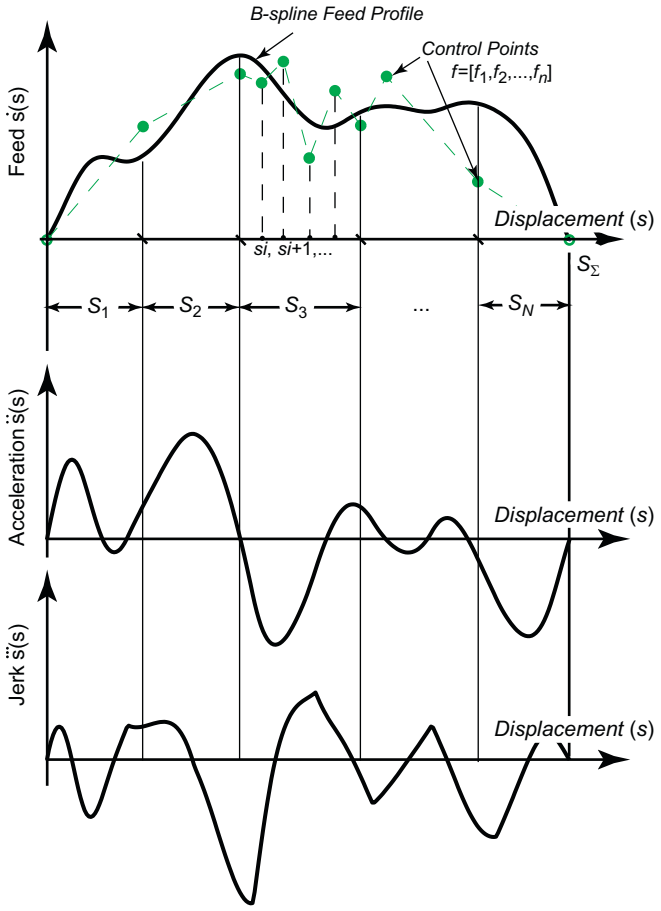

Fig. 1. Feed profile along the tool-path.

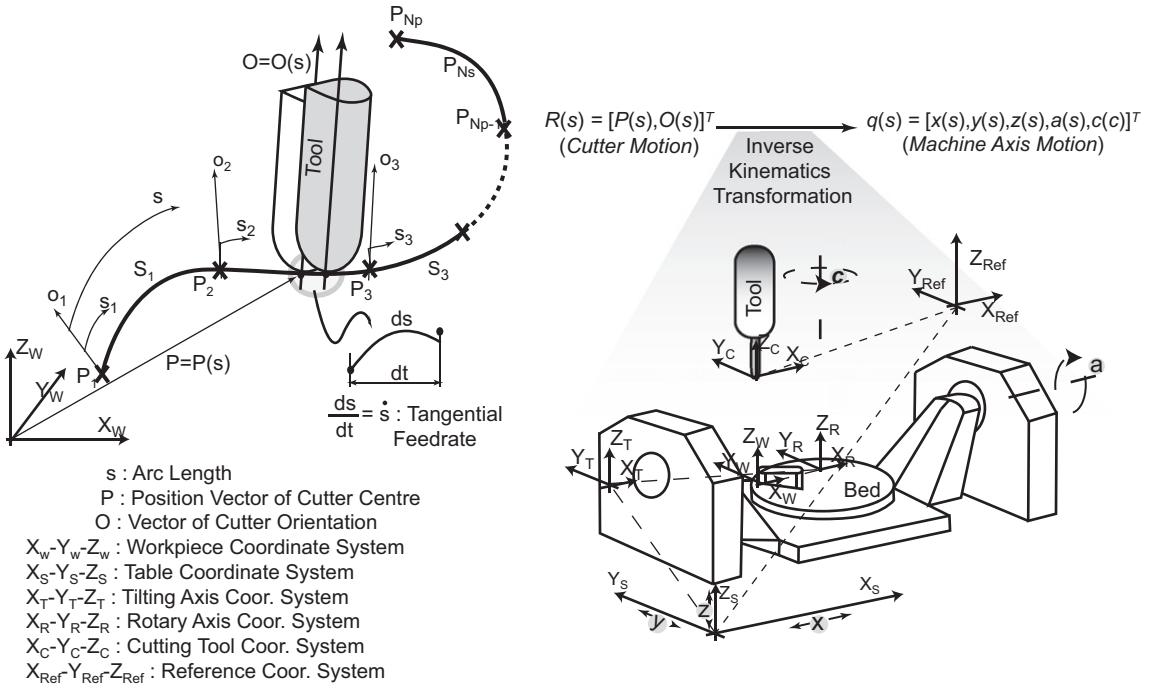

Fig. 2. Five-axis motion generation.

intermediate cutter positions as the tool travels along the path (see Fig. 2). Spline tool-paths are generally parameterized with respect to their length (s) [15]. The tool position and orientation given in the workpiece coordinate system define the pose of the tool expressed as a function of path displacement (s) as

$$R(s) = [P\{P_x(s), P_y(s), P_z(s)\}, \quad O\{O_x(s), O_y(s), O_z(s)\}]^{\mathrm{T}}. \tag{5}$$

The pose is then transformed to axis drive positions as a function of path displacement (s) by the inverse kinematics model of the five-axis machine,

$$\mathbf{q}_{5\times1}(s) = [x(s), y(s), z(s), a(s), c(s)]^{\mathrm{T}}, \tag{6}$$

where $[x(s),\ y(s),\ z(s)]$ and $[a(s),\ c(s)]$ are the positions of linear and rotary drives, respectively. The velocity ($\dot{\mathbf{q}}_{5\times1}$), acceleration ($\ddot{\mathbf{q}}_{5\times1}$) and jerk ($\mathbf{q}^{\mathrm{I}}_{5\times1}$) profiles of each drive are evaluated as,

$$\left.\begin{aligned}\dot{\mathbf{q}}(s) &= \mathbf{q}_s(s)\dot{s}(s)\\ \ddot{\mathbf{q}}(s) &= \mathbf{q}_{ss}(s)\dot{s}^2(s) + \mathbf{q}_s(s)\ddot{s}(s)\\ \mathbf{q}^{\mathrm{I}}(s) &= \mathbf{q}_{sss}(s)\dot{s}^3(s) + 3\mathbf{q}_{ss}(s)\dot{s}(s)\ddot{s}(s) + \mathbf{q}_s(s)\dddot{s}(s)\end{aligned}\right\}, \tag{7}$$

where

$$\left.\mathbf{q}_s(s) = \frac{\mathrm{d}\mathbf{q}(s)}{\mathrm{d}s}, \quad \mathbf{q}_{ss}(s) = \frac{\mathrm{d}^2\mathbf{q}(s)}{\mathrm{d}s^2}, \quad \mathbf{q}_{sss}(s) = \frac{\mathrm{d}^3\mathbf{q}(s)}{\mathrm{d}s^3}\right\} \tag{8}$$

are derivatives of the axis positions.

3. Kinematic and dynamic constraints

The user commands the tool to maintain the feed along the tool-path in order to preserve the allowed chip load on the tool, i.e. $\dot{s} \leqslant$ feed. However, as derivatives of the tool-path changes, the commanded path velocity, the feed, may violate the speed, acceleration and jerk limits of active drives on the five-axis machine tool. The feed must be constrained to avoid the violation of axis limits as follows.

3.1. Velocity constraints

The velocities of five drives given in Eq. (7) must not exceed their saturation limits $[v_{x\,\max}\ \ v_{y\,\max}\ \ v_{z\,\max} v_{a\,\max} v_{c\,\max}]^{\mathrm{T}}$ for a five-axis machine tool traveling along a curved tool-path ($0 \leqslant s \leqslant S_\Sigma$),

$$-\begin{bmatrix}1\\1\\1\\1\\1\end{bmatrix} \leqslant \begin{bmatrix}\dfrac{x_s(s)}{v_{x\,\max}}\\ \dfrac{y_s(s)}{v_{y\,\max}}\\ \dfrac{z_s(s)}{v_{z\,\max}}\\ \dfrac{a_s(s)}{v_{a\,\max}}\\ \dfrac{c_s(s)}{v_{c\,\max}}\end{bmatrix} \dot{s}(s) \leqslant \begin{bmatrix}1\\1\\1\\1\\1\end{bmatrix}. \tag{9}$$

The path velocity is positive $\dot{s}(s) \geqslant 0$, and using the normalized partial derivatives,

$$\mathbf{q}_s^v(s)_{5\times 1} = \left[\frac{x_s(s)}{v_{x\,\max}}, \frac{y_s(s)}{v_{y\,\max}}, \frac{z_s(s)}{v_{z\,\max}}, \frac{a_s(s)}{v_{a\,\max}}, \frac{c_s(s)}{v_{c\,\max}}\right]^{\mathrm{T}} \tag{10}$$

the axis velocities are constrained as,

$$|q_{s,i}^v(s)|\dot{s}(s) - 1 \leqslant 0, \quad i = 1, 2, \ldots, 5. \tag{11}$$

The absolute values of derivatives of the axis positions ($|q_{s,i}^v(s)|$) are expressed as scalar functions of the path length (s), hence they are evaluated from the specified path geometry as shown in Fig. 2. The maximum allowable feed ($\dot{s}_V$), computed from Eq. (11) satisfies the velocity constraints ($[v_{x\,\max} \quad v_{y\,\max} \quad v_{z\,\max} \quad v_{a\,\max} \quad v_{c\,\max}]^{\mathrm{T}}$) of all five drives:

$$\dot{s}_{V,\max}(s) = \frac{1}{\max\limits_{i=1,2,\ldots,5}\{|q_{s,i}^v(s)|\}} = \frac{1}{q_{s,\max}^v}. \tag{12}$$

It is evident from Eqs. (9) and (12) that the drive, which has the maximum first derivative of its displacement normalized with its velocity limit, determines the allowable feed along the path (s). Eq. (12) may also be expressed in a single velocity inequality as:

$$C_v(s) = q_{s,\max}^v \dot{s}(s) - 1 \leqslant 0. \tag{13}$$

3.2. Acceleration constraints

The product of acceleration and reflected inertia at the motor determine the required dynamic torque from the actuator. The torque or equivalent acceleration at each drive must be constrained to avoid actuator saturation limits. If the axis acceleration limits are specified as $[a_{x\,\max} \quad a_{y\,\max} \quad a_{z\,\max} \quad a_{a\,\max} \quad a_{c\,\max}]^{\mathrm{T}}$, the feed ($\dot{s}$) must be constrained according to Eq. (7) as,

$$-\begin{bmatrix} a_{x\,\max} \\ a_{y\,\max} \\ a_{z\,\max} \\ a_{a\,\max} \\ a_{c\,\max} \end{bmatrix} \leqslant \underbrace{\begin{bmatrix} x_{ss}(s) \\ y_{ss}(s) \\ z_{ss}(s) \\ a_{ss}(s) \\ c_{ss}(s) \end{bmatrix}}_{\mathbf{q}_{ss}} \dot{s}^2(s) + \underbrace{\begin{bmatrix} x_s(s) \\ y_s(s) \\ z_s(s) \\ a_s(s) \\ c_s(s) \end{bmatrix}}_{\mathbf{q}_s} \ddot{s}(s) \leqslant \begin{bmatrix} a_{x\,\max} \\ a_{y\,\max} \\ a_{z\,\max} \\ a_{a\,\max} \\ a_{c\,\max} \end{bmatrix} \tag{14}$$

for $0 \leqslant s \leqslant S_\Sigma$. By normalizing the derivatives of the axis positions with the acceleration limits,

$$\left.\begin{aligned} \mathbf{q}_s^a(s) &= \left[\frac{x_s(s)}{a_{x\,\max}}, \frac{y_s(s)}{a_{y\,\max}}, \frac{z_s(s)}{a_{z\,\max}}, \frac{a_s(s)}{a_{a\,\max}}, \frac{c_s(s)}{a_{c\,\max}}\right]^{\mathrm{T}} \\ \mathbf{q}_{ss}^a(s) &= \left[\frac{x_{ss}(s)}{a_{x\,\max}}, \frac{y_{ss}(s)}{a_{y\,\max}}, \frac{z_{ss}(s)}{a_{z\,\max}}, \frac{a_{ss}(s)}{a_{a\,\max}}, \frac{c_{ss}(s)}{a_{c\,\max}}\right]^{\mathrm{T}} \end{aligned}\right\} \tag{15}$$

Eq. (14) is reduced to the following form

$$|q_{ss,i}^a(s)\dot{s}^2(s) + q_{s,i}^a(s)\ddot{s}(s)| \leqslant 1, \quad i = 1, 2, \ldots, 5. \tag{16}$$

Using the triangular ($|A + B| \leqslant |A| + |B|$) and multiplicative ($|A \times B| \leqslant |A| \times |B|$) properties of the absolute value, the acceleration inequalities may be expanded as:

$$|q_{ss,i}^a(s)|\dot{s}^2(s) + |q_{s,i}^a(s)||\ddot{s}(s)| \leqslant 1, \quad i = 1, 2, \ldots, 5. \tag{17}$$

Note that Eq. (17) represents a linear relationship between square of the feed ($\dot{s}^2$) and the tangential acceleration ($\ddot{s}$) for each axis ($\mathbf{q}(s) = [x(s), y(s), z(s), a(s), c(c)]^{\mathrm{T}}$) (see Fig. 3). When the machine starts to move from zero speed, it can use the maximum allowable tangential acceleration to reach the desired feed, which corresponds to ($\ddot{s}$) axis. When the machine travels at the constant feed ($\dot{s}$), the required tangential acceleration is zero. The acceleration limits of the drives determine the allowable feed and tangential acceleration. While one axis may limit the feed, another may constrain the acceleration depending on their partial derivatives. A pair of feed and tangential acceleration must be

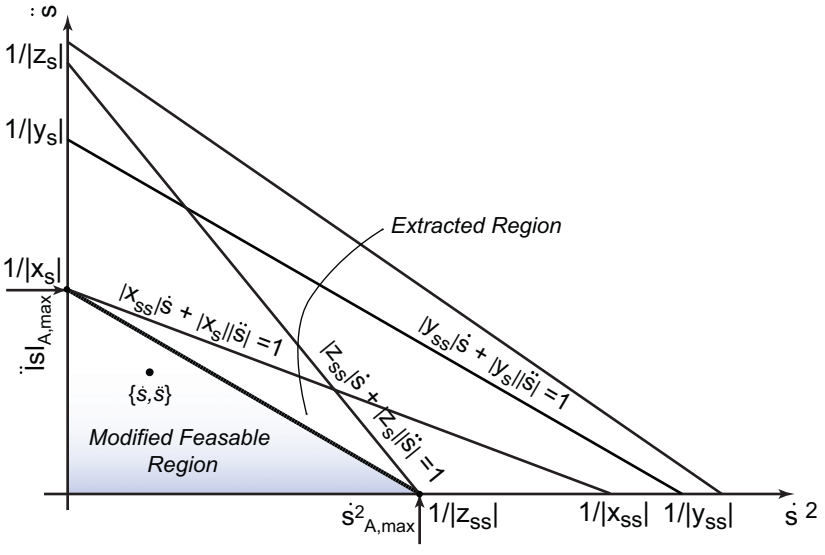

Fig. 3. Modified, acceleration feasible operating region.

identified iteratively during feed optimization from the five sets of inequalities to avoid violating the acceleration limits of the drives which leads to the acceleration feasible operating region of the machine given at a path position (s) as in Fig. 3.

However, the iterative solution of feasible feed and acceleration may bring unaffordable computational cost to the real time trajectory generation algorithm. The feasible solution region for the feed and tangential acceleration may be bounded by the acceleration limits of only a few drives as illustrated in Fig. 3, and evaluated from,

$$\left.\begin{aligned}\dot{s}(s)=0\Rightarrow \ddot{s}_{A,\max}(s)&=\min_{i=1,2,\ldots,5}\left\{\frac{1}{|q^a_{s,i}(s)|}\right\}\\&=\left\{\frac{1}{\max\limits_{i=1,2,\ldots,5}|q^a_{s,i}(s)|}\right\}=\frac{1}{q^a_{ss,\max}(s)}\\ \ddot{s}(s)=0\Rightarrow \dot{s}_{A,\max}(s)&=\min_{i=1,2,\ldots,5}\left\{\sqrt{\frac{1}{|q^a_{ss,i}(s)|}}\right\}\\&=\left\{\sqrt{\frac{1}{\max\limits_{i=1,2,\ldots,5}|q^a_{ss,i}(s)|}}\right\}=\frac{1}{q^a_{s,\max}(s)}\end{aligned}\right\}. \tag{18}$$

By substituting $(q^a_{s,\max}, q^a_{ss,\max})$, Eq. (17) can be reduced to a simple linear relationship defining a triangular, feasible feed and tangential acceleration region bound by $(\dot{s}_{A,\max}, \ddot{s}_{A,\max})$,

$$C_a(s)=q^a_{s,\max}(s)|\ddot{s}(s)|+q^a_{ss,\max}(s)\dot{s}^2(s)-1\leqslant 0. \tag{19}$$

Eq. (19) reduces the computational cost of the iterative feed optimization procedure by cutting down the number of constraint evaluations from five (Eq. (17)) to one at the expense of losing part of the feasible feed-acceleration region as shown in Fig. 3.

3.3. Jerk constraints

Limiting the axis jerk values smooth, the position commands; hence reducing the high frequency content, which leads to a better tracking performance along the curved path. If the imposed jerk limits are $[J_{x\max}\quad J_{y\max}\quad J_{z\max}\quad J_{a\max}\quad J_{c\max}]^{\mathrm{T}}$, the following normalized jerk constraints are defined from Eq. (7):

$$-\begin{bmatrix}1\\1\\1\\1\\1\end{bmatrix}\leqslant\underbrace{\begin{bmatrix}\frac{x_{sss}(s)}{J_{x\max}}\\ \frac{y_{sss}(s)}{J_{y\max}}\\ \frac{z_{sss}(s)}{J_{z\max}}\\ \frac{a_{sss}(s)}{J_{a\max}}\\ \frac{c_{sss}(s)}{J_{c\max}}\end{bmatrix}}_{\mathbf{q}^j_{sss}(s)}\dot{s}^3(s)+3\underbrace{\begin{bmatrix}\frac{x_{ss}(s)}{J_{x\max}}\\ \frac{y_{ss}(s)}{J_{y\max}}\\ \frac{z_{ss}(s)}{J_{z\max}}\\ \frac{a_{ss}(s)}{J_{a\max}}\\ \frac{c_{ss}(s)}{J_{c\max}}\end{bmatrix}}_{\mathbf{q}^j_{ss}(s)}\dot{s}(s)\ddot{s}(s)$$

$$+\underbrace{\begin{bmatrix}\frac{x_s(s)}{J_{x\max}}\\ \frac{y_s(s)}{J_{y\max}}\\ \frac{x_s(s)}{J_{z\max}}\\ \frac{x_s(s)}{J_{a\max}}\\ \frac{x_s(s)}{J_{c\max}}\end{bmatrix}}_{\mathbf{q}^j_{s}(s)}\dddot{s}(s)\leqslant\begin{bmatrix}1\\1\\1\\1\\1\end{bmatrix} \tag{20}$$

for $0\leqslant s\leqslant S_\Sigma$. Alternatively, Eq. (20) can be expressed by,

$$|q^j_{sss,i}(s)\dot{s}^3(s)+3q^j_{ss,i}(s)\dot{s}(s)\ddot{s}(s)+q^j_{s,i}(s)\dddot{s}(s)|\leqslant 1,\quad i=1,2,\ldots,5 \tag{21}$$

and expanded as

$$|q^j_{sss,i}(s)||\dot{s}^3(s)|+3|q^j_{ss,i}(s)||\dot{s}(s)||\ddot{s}(s)|+|q^j_{s,i}(s)||\dddot{s}(s)|\leqslant 1,\quad i=1,2,\ldots,5. \tag{22}$$

where $|q^j_{sss,i}(s)|$, $|q^j_{ss,i}(s)|$ and $|q^j_{s,i}(s)|$ are tool-path dependent derivatives. Eq. (22) generates a three dimensional operating surface with respect to the jerk limits of the drives as shown in Fig. 4. The maximum feed ($\dot{s}$), tangential acceleration ($\ddot{s}$) and the jerk ($\dddot{s}$) at a path position (s) can be identified by setting two of them to zero, and evaluating the other from the jerk limits of the drives. For instance, the jerk limited maximum feed ($\dot{s}_{J,\max}(s)$) is computed as,

$$\ddot{s}(s)=\dddot{s}(s)=0\Rightarrow \dot{s}_{J,\max}(s)=\min_{i=1,2,\ldots,5}\left\{\sqrt[3]{\frac{1}{|q^j_{sss,i}(s)|}}\right\}. \tag{23}$$

The feasible set of feed, tangential acceleration and jerk identified in the operating region is then iteratively found during feed optimization by evaluating Eq. (22), which is computationally complex and too costly to be implemented in a CNC system. Similar to the methodology presented for the acceleration limits, the maximum values of the jerk normalized derivatives are selected by considering all five drives,

$$\left.\begin{aligned}q^j_{sss,\max}(s)&=\max_{i=1,2,\ldots,5}\{|q^j_{sss,i}(s)|\}\\ q^j_{ss,\max}(s)&=\max_{i=1,2,\ldots,5}\{|q^j_{ss,i}(s)|\}\\ q^j_{s,\max}(s)&=\max_{i=1,2,\ldots,5}\{|q^j_{s,i}(s)|\}\end{aligned}\right\} \tag{24}$$

and substituted in Eq. (22) to find the constraint equation,

$$C_j(s)=q^j_{sss,\max}(s)\dot{s}^3(s)+3q^j_{ss,\max}(s)\dot{s}(s)|\ddot{s}(s)|+q^j_{s,\max}(s)|\dddot{s}(s)|-1\leqslant 0. \tag{25}$$

While Eq. (22) has to be evaluated for all five axes, Eq. (25) is a single set, which considers a combination of axes whose jerk limits affect the feasible operating region of the

machine tool. However, the tangential jerk, acceleration and speed are still coupled; hence they need to be identified iteratively from Eq. (25). The identified feed ($\dot{s}_J(s)$), tangential acceleration ($\ddot{s}_J(s)$) and tangential jerk ($\dddot{s}_J(s)$) satisfy the jerk limits on all five drives.

4. Solution of minimum time feed optimization problem

It is proposed that the feed is scheduled along the tool-path without violating the velocity, acceleration and jerk limits of all five drives. The axes constraints given in Eqs. (13), (19) and (25) are stacked into the following vector

$$\mathbf{C}(s) = [\, C_f^-(s) \quad C_f^+(s) \quad C_v(s) \quad C_a(s) \quad C_j(s) \,]^{\mathrm{T}}_{5\times 1}, \tag{26}$$

where $C_f^-(s) = -\dot{s}(s) \leqslant 0$ is the lower limit of the velocity to ensure forward motion (e.g. positive feed direction), and $C_f^+(s) = \dot{s}(s) - \text{feed} \leqslant 0$ is the user specified upper limit of the feed along the path. Hence, the feed at any position along the five-axis tool-path must satisfy the drive constraints by selecting the most conservative value,

$$\dot{s} \leqslant \min\{\dot{s}_V(s), \dot{s}_A(s,\ddot{s}), \dot{s}_J(s,\ddot{s},\dddot{s})\}. \tag{27}$$

The feed is limited by one of the velocity, acceleration and jerk limits of the drives along different sections of the tool-path. The algorithm identifies allowable feed, tangential acceleration and jerk at each tool position along the path. When the feed is varied between the two consecutive tool-path points, the corresponding tangential acceleration and jerk must be less than the values already set by the drive limits at the target tool-path point.

$$|\ddot{s}| \leqslant \min\{\ddot{s}_A(s,\dot{s}), \ddot{s}_J(s,\dot{s},\dddot{s})\}, \quad |\dddot{s}| \leqslant \min\{\dddot{s}_J(s,\dot{s},\ddot{s})\}. \tag{28}$$

The feed optimization problem is defined as the minimization of tool-path travel time while respecting the velocity, acceleration and jerk constraints of all five axes along the tool-path. The nonlinear optimization is solved using Sequential Quadratic Problem (SQP) [16]. The feed profile is expressed in B-spline form as a function of path length (s) with modulated control points ($\mathbf{f}$) defined at n fixed path

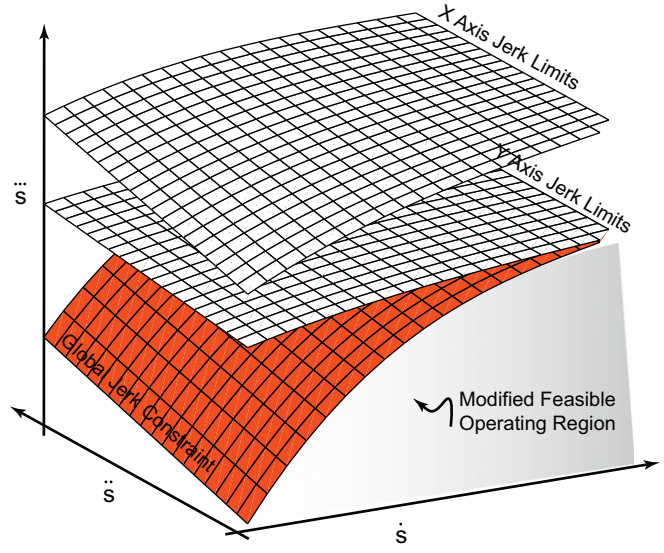

Fig. 4. Jerk feasible operating region.

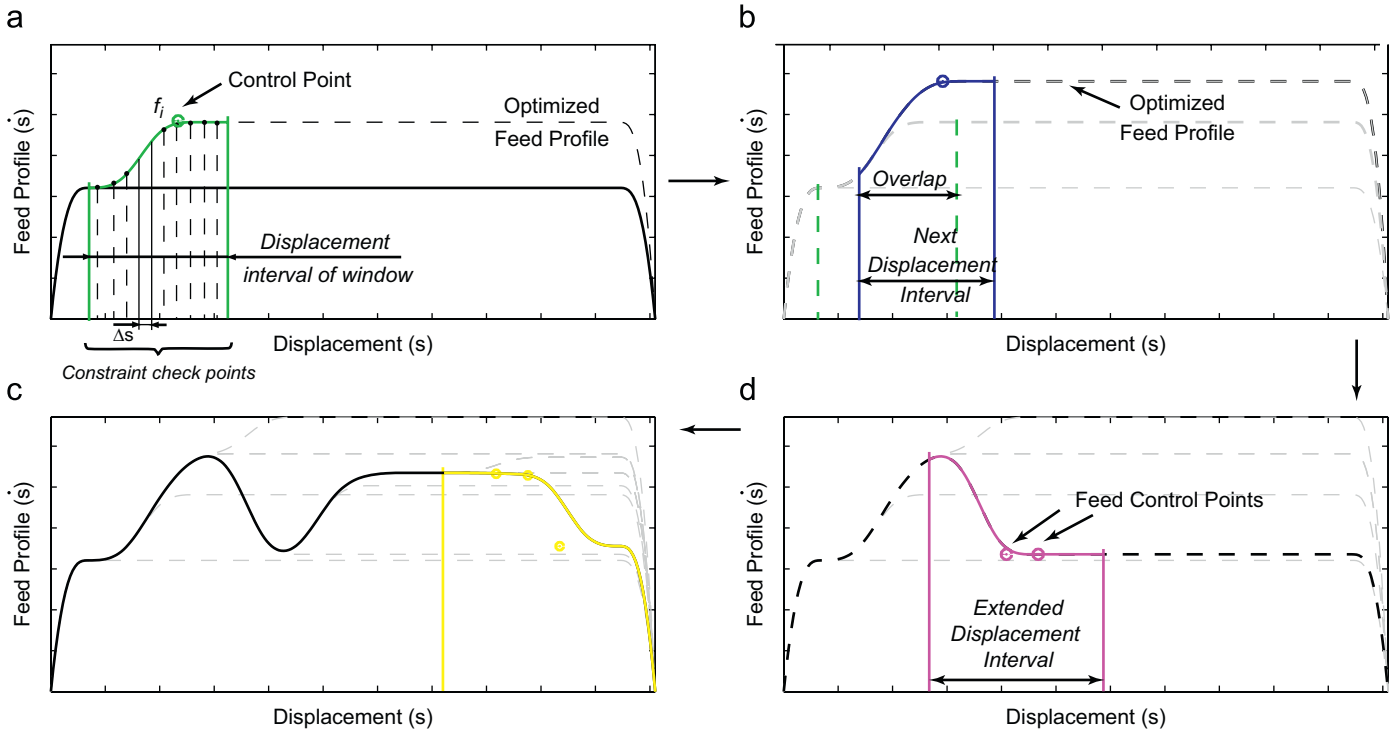

Fig. 5. Windowing approach. (a) Forward windowing (start), (b) forward windowing (shifted…), (c) forwarding windowing (finalized) and (d) forward windowing (extended…).

positions (**s**),

$$\mathbf{f} = [f_0, f_1, \ldots, f_{n-1}], \quad \mathbf{s} = [s_0, s_1, \ldots, s_{n-1}] \tag{29}$$

and optimized to minimize the machining time while respecting axis constraints (**C**(s)) given in Eq. (26)

$$J = \min_{f} \int_0^S \frac{\mathrm{d}s}{\dot{s}} \quad \text{subject to :} \quad \mathbf{C}(s) \leqslant 0 \quad \text{for } 0 \leqslant s \leqslant S_\Sigma, \tag{30}$$

While the feed control points (**f**) are fixed at (n) path points (**s**), the violation of constraints can be checked at denser intervals (Δs ($\sim$0.1, …, 1) mm). The fixed number feed control points move up and down, altering the feed profile during the iterative optimization process until optimal nominal feed values, which do not violate the machine drive constraints, are obtained.

The optimization process can be computationally inefficient if all control points are considered simultaneously along a long tool-path. Instead, the optimization algorithm is applied in moving windows with a smaller number of control points (i.e. 20). The overlapping part of the window can be limited to few points (i.e. 5) depending on the sharp changes in the curvature of the path as shown in Fig. 5.

5. Simulation and experimental results

The proposed trajectory optimization algorithm is applied to five-axis flank milling of a jet engine impeller, and the tool-path is shown in Fig. 6. The machine tool shown in Fig. 7 has three cartesian (x,y,z) and two rotary (a,c) drives with 2.9 μm and 0.0005° encoder resolutions, respectively. The in house developed research CNC has an open architecture, which allows rapid implementation of trajectory generation and control laws. The tool-path for one impeller blade consists of 196 positions at varying displacement intervals, and is fitted with a B-spline at the tool tip ($P(s)$) with a chord error of 35 μm and the orientation error of 0.09°. The programmed feed along the path was 150 mm/s.

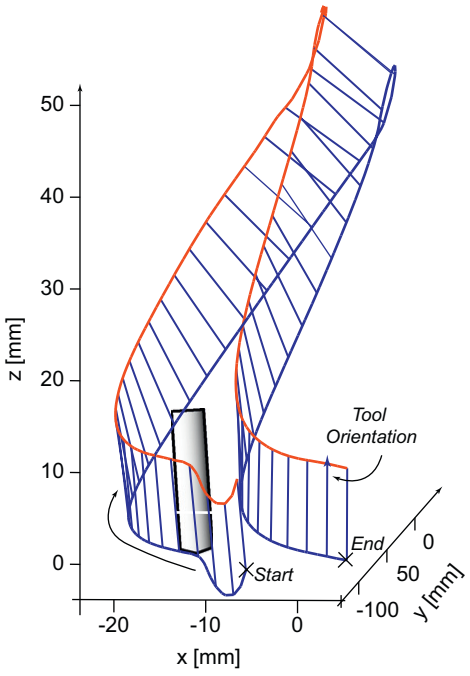

Fig. 6. Multi-axis tool-path.

The curvature along the tool-path changes continuously, but with worst peaks at the beginning (25–50 mm), in the middle (150–190 mm), and towards the end (250–290 mm) where the tool has to move around the trailing and leading edges of the blade. The transformation of tool position into the axis positions is summarized as:

$$\left.\begin{aligned}
c(s) &= \tan^{-1}\left(\frac{O_x(s)}{O_y(s)}\right),\\
a(s) &= \tan^{-1}\left(\frac{\sqrt{O_x^2(s)+O_y^2(s)}}{O_y(s)}\right),\\
x(s) &= -P_x(s)\cos(c(s)) + P_y(s)\sin(c(s)),\\
y(s) &= -\cos(a(s))\sin(c(s))P_x(s) - \cos(a(s))\\
&\quad \times \cos(c(s))P_y(s) + \sin(a(s))P_z(s),\\
z(s) &= -(-\sin(a(s))\sin(c(s))P_x(s) - \sin(a(s))\\
&\quad \times \cos(c(s))P_y(s) - \cos(a(s))P_z(s))
\end{aligned}\right\}. \tag{31}$$

The corresponding axis positions ($\mathbf{q}_{5\times1}(s) = [x(s),\ y(s),\ z(s),\ a(s),\ c(s)]$) along the 300 mm long tool-path are shown in Fig. 8. The two linear ($x(s)$, $y(s)$) and one rotary ($c(s)$) drive displacements show sharp changes at the high curvature locations.

The axis limits of the machine are given in Table 1. The drives are controlled by a robust sliding mode controller with feed-forward friction compensation presented by Altintas et al. [17].

The path velocities constrained by each drive velocity, acceleration and jerk limits are evaluated from Eqs. (12), (18) and (23) and shown in Fig. 9. Depending on the curvature of the path, different drives limit the feed, along the tool-path. For example, x-axis limits the maximum feed at $\dot{s} = 58$ mm/s at path position ($s = 34$ mm), and y and c drives limit the feed at path location ($s = 267$ mm/s). Similarly, the acceleration and jerk limits of the drives constrain the feed at different locations of the path. The envelope, that passes through minimum feeds limited by the velocity (Fig. 9a), acceleration (Fig. 9b) and jerk (Fig. 9c) are evaluated along the path. The global optimization of the feed cannot combine the three envelopes, since a change in the velocity between two path points may violate the acceleration and jerk limits of the drives. The optimal feed is evaluated by simultaneously optimizing velocity, acceleration and jerk limits of all five drives as given in Eqs. (13), (19) and (25). The identified feed is limited to 150 mm/s set by the process planner, and the resulting feed schedule along the path is given in Fig. 10.

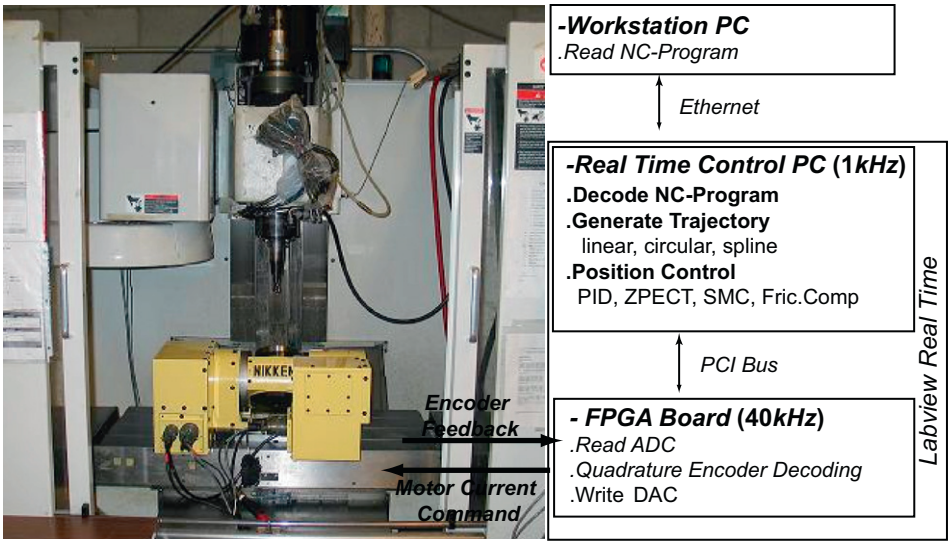

Fig. 7. Experimental open architecture research five-axis CNC.

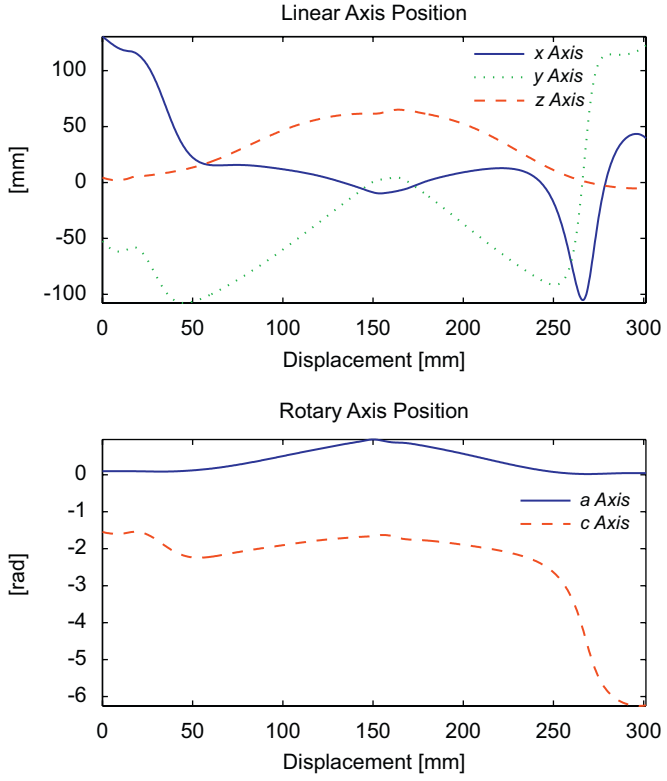

Fig. 8. Axis position profiles.

Table 1
Machine tool drive limits used in optimization of feed

Drives	Velocity (unit/s)	Acceleration (unit/s^2)	Jerk (unit/s^3)
x (mm)	250	2000	3000
y (mm)	250	2000	3000
z (mm)	250	2000	3000
a (°)	166	2500	250
c (°)	290	2000	200

The cruise feed and tangential acceleration are set to $\dot{s} = 150$ mm/s and $\ddot{s} = 1000$ mm/s, respectively.

It can be seen from Fig. 10 that if the machine travels at 150 mm/s, the drive limits are violated at path regions (0–60 mm; 140–165 mm; 240–300 mm) where the curvatures of the impeller blade are sharp. Although modern controller adjust the speed along the sharp curvatures by using look-ahead function, a worst case scenario is used here as an illustration. If the feed is kept constant at 15 mm/s, none of the drive limits are violated but the machining time becomes $T_\Sigma = 20.18$ s. When the feed is optimally scheduled by fitting a B-spline to 274 equally spread points along the tool-path, the machining time drops to $T_\Sigma = 4.664$ s, resulting in an 80% increase in productivity. The algorithm was solved in MATLAB [16] environment in 126 s on a P4 computer with 2.3 GHz CPU speed. As shown in Fig. 11, the scheduled feed has been tested on the experimental five-axis machine, and the resulting velocity, acceleration and jerk on each drive did not violate their limits.

In addition to the reduction in machining time, the proposed optimization improves the tracking accuracy of the machine when the drives are not saturated. The experimentally measured tracking errors are shown in Fig. 12 for three cases. When the feed is set to the most conservative feed (15 mm/s), the drive limits are never violated, the tracking accuracy is best due to the slow speed but the machining time becomes $T_\Sigma = 20.18$ s. If the user imposed feed (150 mm/s) was used, the drives become saturated excessively and the machine becomes uncontrollable. A relatively conservative feed of $f = 40$ mm/s was tested, which led to the violation of drive limits (Fig. 12)

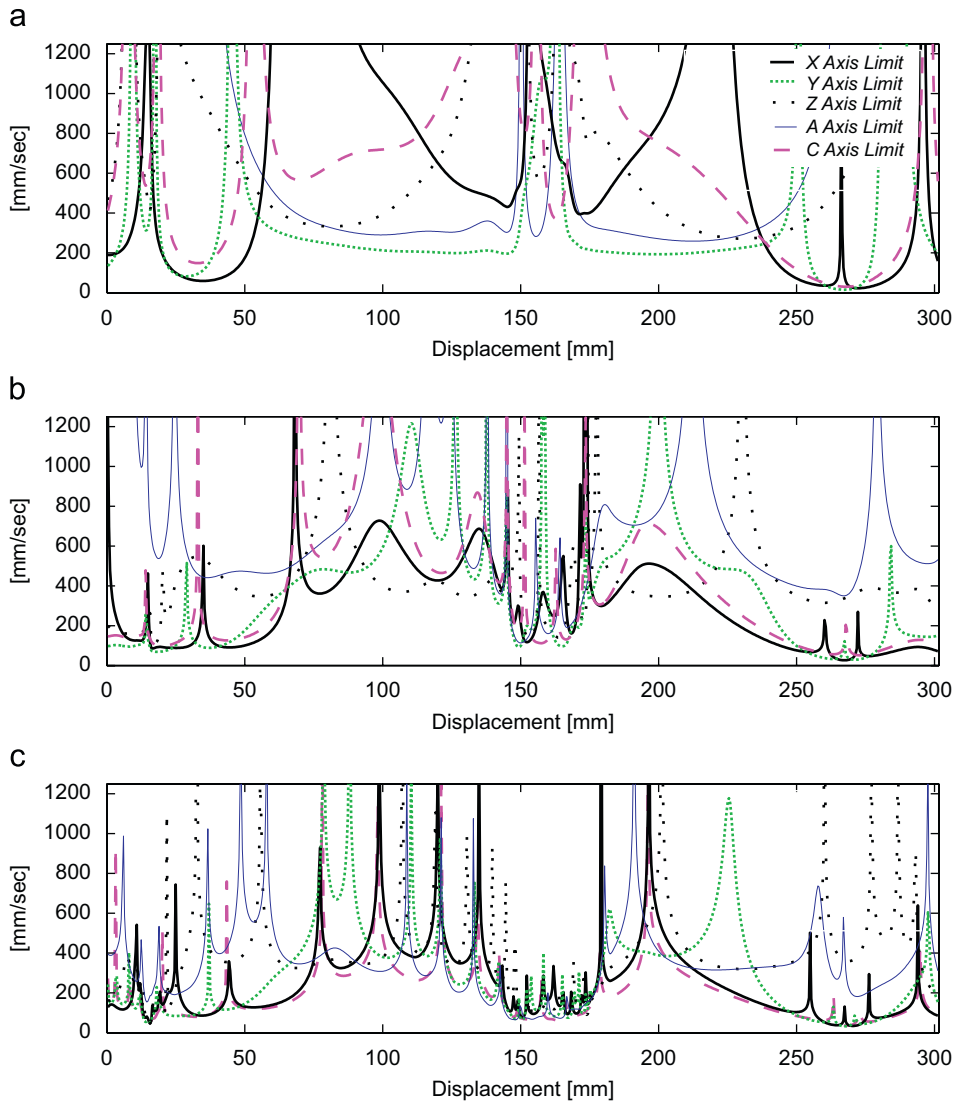

Fig. 9. Feed limits with respect to axis velocity constraints. (a) Feedrate limited by the axis velocity constraints, (b) feedrate limited by the axis acceleration constraints and (c) feedrate limited by the axis jerk constraints.

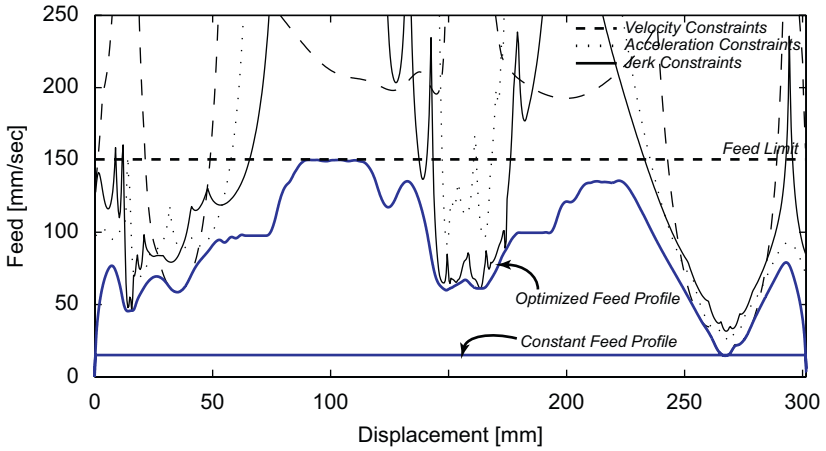

Fig. 10. Optimized and un-optimized feed profiles.

and the tracking errors are amplified at the saturation regions along the path. However, when the feed is optimized, the machine was able to reach up to the desired feed of 150 mm/s at most locations, and the drive limits were never violated. The machine tool control was kept in a linear control region and the tracking accuracy became

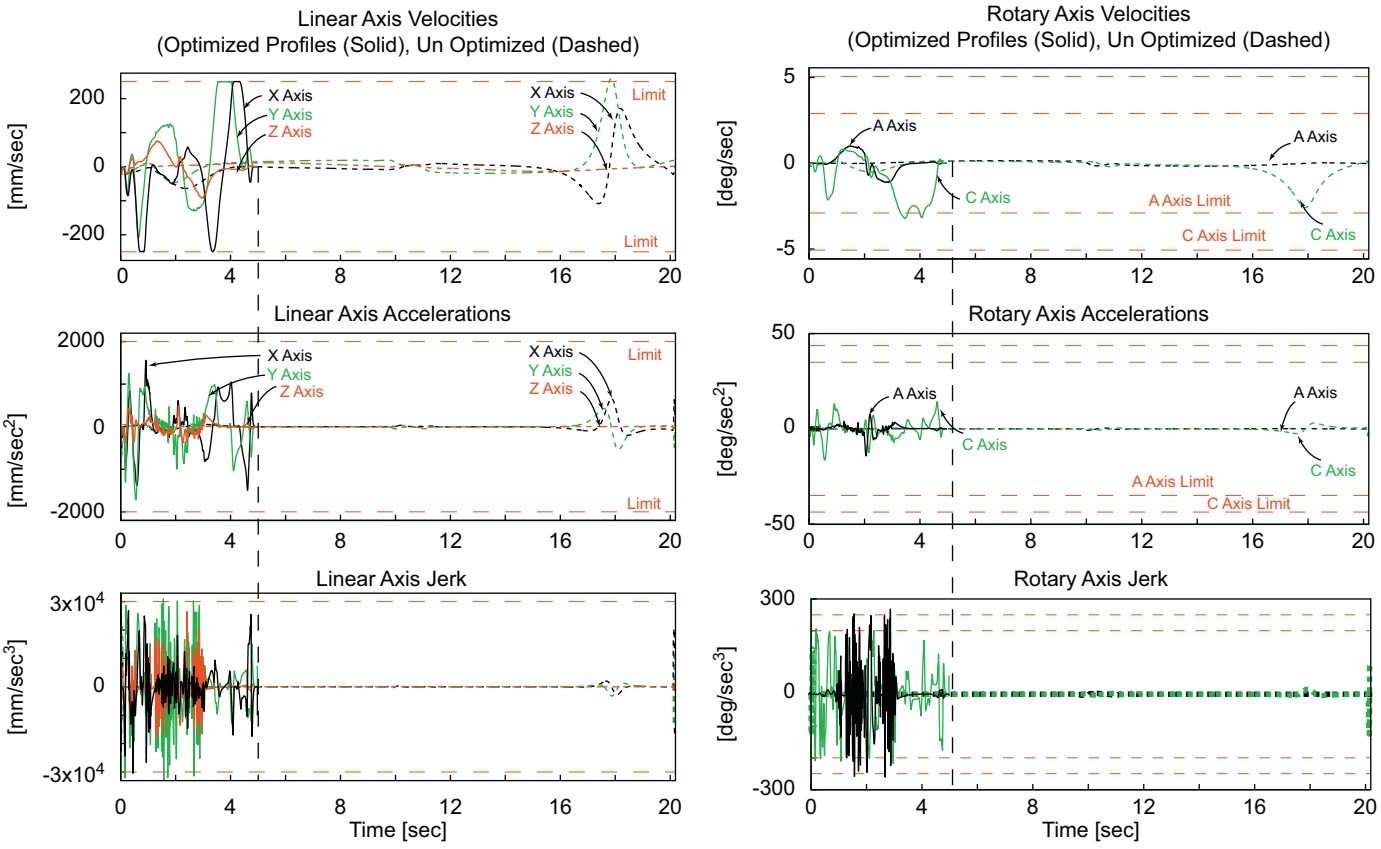

Fig. 11. Axis profiles.

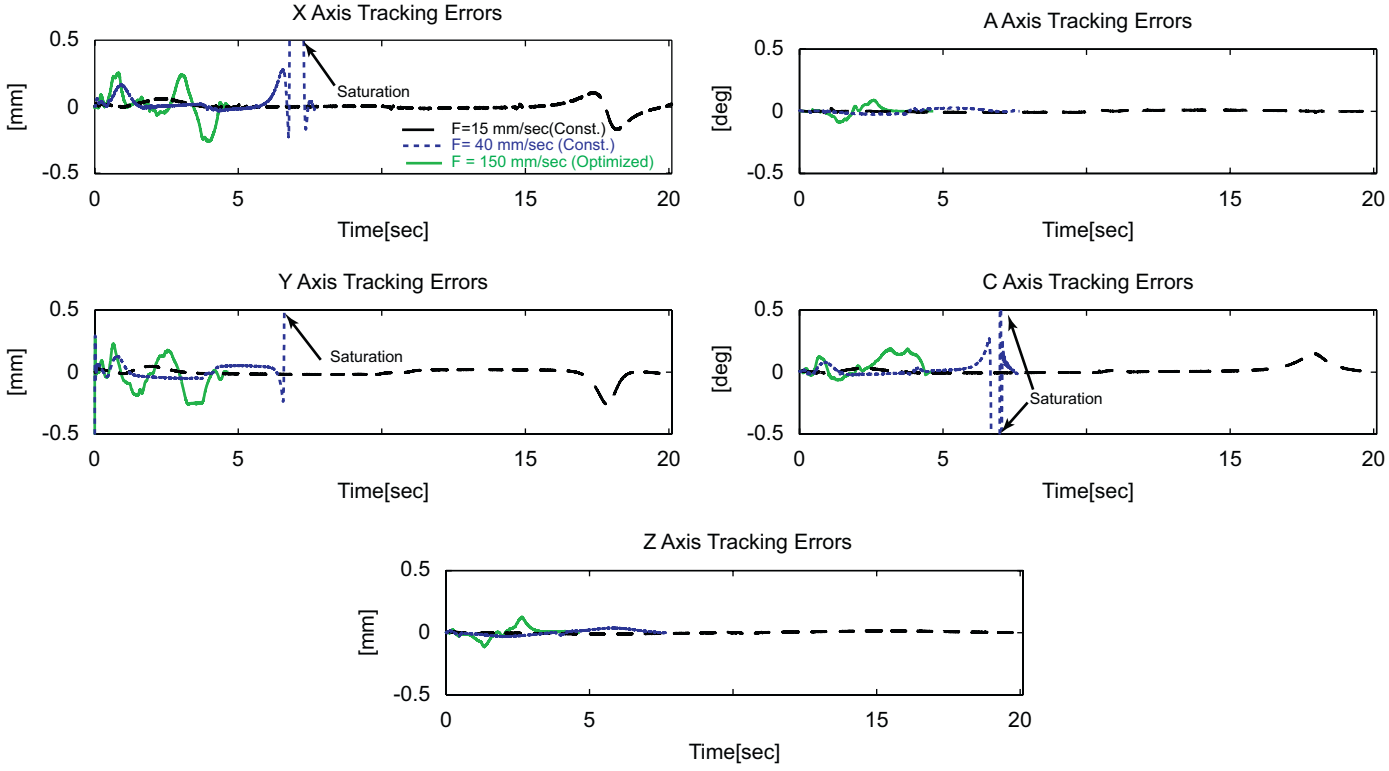

Fig. 12. Tracking errors.

linearly proportional to the velocities and inversely proportional to the bandwidth of the drives.

6. Conclusions

The productivity of five-axis machining of dies, molds and aerospace parts with sculptured surfaces is hindered by the metal cutting process, the machine tool's structural dynamics, thermal and volumetric accuracy of the machine, and kinematics and control of the drives. This paper showed that the machining time can be significantly reduced by optimizing the feed along the tool-path while respecting velocity, acceleration and jerk limits of all five drives. In addition, the avoidance of violating the saturation limits of the drives allows the control law to operate in a linear region, hence improving the accuracy and performance of the CNC system. The tangential feed along the cutter axis varies when the axial depth of cut is long, leading to conflicting velocity, acceleration and jerk demands at each drive. The proposed algorithm can be repeated along the cutter axis, and the feed which satisfies the drive constraints can be selected.

Acknowledgments

This research is supported by the National Science and Engineering Research Council of Canada and Pratt & Whitney Canada, under the Industrial Research Chair program.

Appendix. Feed profile generated with a B-spline

A cubic B-spline is used to smooth the scheduled feed, providing a jerk continuous (C^3) feed profile ($\dot{s} = s(s)$) along the tool-path as illustrated in Fig. 1. The B-spline feed profile is defined by specifying nominal feed values, $\mathbf{f} = [f_0, f_1, \ldots, f_{n-1}]$ at fixed feed modulation points along the path length, $\mathbf{s} = [s_0^p, s_1^p, \ldots, s_{n-1}^p]$. The nominal feeds are evaluated from the velocity, acceleration and jerk limits expressed in Sections 3.1, 3.2 and 3.3. The discrete nominal feed points ($\mathbf{f}$) are then assigned as control points to fit a cubic B-spline, that defines the jerk continuous feed profile along the tool-path ($0 \leqslant s \leqslant S_\Sigma$). Each tool-path segment between two geometric points (R_k, R_{k+1}) is divided into m equal arc-length segments to improve the optimization of the feed variation while respecting the axis constraints. The number of control points becomes $n = mN_s$ where N_s is the original number of segments specified in the NC tool-path. The feed profile ($\dot{s}$) is expressed in B-spline form as:

$$\begin{aligned}\dot{s}(u) &= N_{0,3}(u)f_0 + N_{1,3}(u)f_1 + \cdots + N_{n-1,3}(u)f_{n-1} \\ &= \sum_{i=0}^{n-1} N_{i,3}(u)f_i. \end{aligned} \tag{A.1}$$

$u \in [0,1]$ is the feed profile parameter normalized with respect to the total path length (S_Σ),

$$u = s\frac{1}{S_\Sigma}. \tag{A.2}$$

Note that, the B-spline (Eq. (A.1)) interpolates the nominal feed points f_i with respect to n sets of cubic interpolation functions, $N_{i,3}(u)$, that are computed discretely through evaluation of the following recurrence formula,

$$\left.\begin{aligned} N_{i,0}(u) &= \begin{cases} 1, & \text{if } u_i \leqslant u \leqslant u_{i+1}, \\ 0, & \text{otherwise.} \end{cases} \\ N_{i,k}(u) &= \frac{u-u_i}{u_{i+1}-u_i}N_{i,k-1}(u) + \frac{u_{i+4}-u}{u_{i+4}-u_{i+1}}N_{i+1,k-1}(u) \end{aligned}\right\}, \quad k = 1,2,3. \tag{A.3}$$

The interpolation functions ($N_{i,3}(u)$) are dependent only on uniformly distributed path displacements (u), hence the B-spline parameters do not change when the feeds are altered up and down during the axis-constraint based optimization. The parameter vector ($\mathbf{u}$) contains $n-2$ uniformly distributed B-spline parameters along the entire tool-path and computed as

$$\mathbf{u} = [\,0 \quad u_1 \quad u_2 \quad \ldots \quad 1\,] = [\underbrace{0 \quad \Delta s \quad 2\Delta s \quad \ldots \quad S_\Sigma}_{n-2 \text{ points}}] \times \frac{1}{S_\Sigma}, \quad \text{where } \Delta s = \frac{S_\Sigma}{n-3}. \tag{A.4}$$

In order to force the B-spline to pass through initial and final feed points [($s = 0$, $f_0 = f_{\text{init}}$) and ($s = S_\Sigma$, $f_{n-1} = f_{\text{final}}$)], the first and last entries in the parameter vector ($\mathbf{u}$) are repeated,

$$\mathbf{u} = \left[\underbrace{0 \ldots 0}_{4} \quad u_i \quad u_{i+1} \quad \ldots \quad \underbrace{1 \ldots 1}_{4}\right]. \tag{A.5}$$

The 1st and 2nd derivatives of the feed B-spline with respect to the normalized spline parameter (u) is

$$\left.\begin{aligned} \dot{s}(u) &= \frac{\mathrm{d}s(u)}{\mathrm{d}u} = \frac{\mathrm{d}N_{0,3}(u)}{\mathrm{d}u}f_0 + \cdots + \frac{\mathrm{d}N_{n-1,3}(u)}{\mathrm{d}u}f_{n-1} \\ &= \sum_{i=0}^{n-1}\left(\frac{\mathrm{d}N_{i,3}(u)}{\mathrm{d}u}f_i\right) \\ \ddot{s}(u) &= \frac{\mathrm{d}^2 s(u)}{\mathrm{d}u^2} = \frac{\mathrm{d}^2 N_{0,3}(u)}{\mathrm{d}u^2}f_0 + \cdots + \frac{\mathrm{d}^2 N_{n-1,3}(u)}{\mathrm{d}u^2}f_{n-1} \\ &= \sum_{i=0}^{n-1}\left(\frac{\mathrm{d}^2 N_{i,3}(u)}{\mathrm{d}u^2}f_i\right) \end{aligned}\right\} \tag{A.6}$$

where derivatives of the blending functions are evaluated through repeated differentiation as,

$$\frac{\mathrm{d}^{(k)}N_{i,3}(u)}{\mathrm{d}u^{(k)}} = 3\left(\frac{\mathrm{d}^{(k-1)}N_{i,2}(u)/\mathrm{d}u^{(k-1)}}{u_{i+3}-u_i} - \frac{\mathrm{d}^{(k-1)}N_{i+1,2}(u)/\mathrm{d}u^{(k-1)}}{u_{i+4}-u_{i+1}}\right), \quad k = 1,2. \tag{A.7}$$

Hence, acceleration ($\ddot{s}$) and jerk ($\dddot{s}$) profiles along the path displacement (s) may be evaluated using Eqs. (A.6)

and (A.7) as:

$$\left.\begin{aligned}\ddot{s}(s) &= \left(\frac{1}{S_\Sigma}\right)\left(\dot{s}(u)\frac{\mathrm{d}\dot{s}(u)}{\mathrm{d}u}\right)\Big|_{u=s/S_\Sigma}\\ \dddot{s}(s) &= \left(\frac{1}{S_\Sigma}\right)^2\left(\dot{s}^2(u)\frac{\mathrm{d}^2\dot{s}(u)}{\mathrm{d}u^2}\right)\Big|_{u=s/S_\Sigma}\\ &\quad+\left(\left(\frac{1}{S_\Sigma}\right)\left(\dot{s}(u)\frac{\mathrm{d}\dot{s}(u)}{\mathrm{d}u}\right)\Big|_{u=s/S_\Sigma}\right)^2\end{aligned}\right\}. \tag{A.8}$$

References

[1] J.E. Bobrow, S. Dubowsky, J. Gibson, Time-optimal control of robotic manipulators along specified paths, International Journal of Robotics Research 4 (1985) 3–17.

[2] K. Shin, N. McKay, Minimum-time control of robotic manipulators with geometric path constraints, IEEE Transactions on Automatic Control 30 (1985) 531–541.

[3] Z. Shiller, H.H. Lu, Robust computation of path constrained time optimal motions, in: IEEE International Conference on Robotics and Automation, vol. 1, Cincinnati, OH, May 13–18, IEEE Computer Society Press, Los Alamitos, CA, 1990, pp. 144–149.

[4] Z. Shiller, H.H. Lu, Computation of path constrained time optimal motions with dynamic singularities, ASME Journal of Dynamic System, Measurement, and Control 114 (1992) 34–40.

[5] K. Shin, N. McKay, A dynamic programming approach to trajectory planning of robotic manipulators, IEEE Transactions on Automatic Control 31 (1986) 491–500.

[6] R. Gourdeau, H.M. Schwartz, Optimal control of a robot manipulator using a weighted time-energy cost function, in: IEEE Conference on Decision and Control, vol. 2, Tampa, FL, December 13–15, IEEE, Piscataway, NJ, 1989, pp. 1628–1631.

[7] T.S. Smith, R.T. Farouki, S.D. Timar, G.L. Boyadjieff, Algorithms for time-optimal control of CNC machines along curved tool-paths, Robotics and Computer-Integrated Manufacturing 21 (2005) 37–53.

[8] D. Renton, M.A. Elbestawi, High speed servo control of multi-axis machine tools, International Journal of Machine Tools and Manufacture 40 (2000) 539–559.

[9] J. Dong, J.A. Stori, A generalized time-optimal bidirectional scan algorithm for constrained feedrate optimization, Journal of Dynamic Systems, Measurement and Control, Transactions of the ASME 128 (2) (2006) 379–390.

[10] M. Tarkiainen, Z. Shiller, Time optimal motions of manipulators with actuator dynamics, in: IEEE International Conference on Robotics and Automation, vol. 2, Atlanta, GA, May 2–6, IEEE Comput. Soc. Press, Los Alamitos, CA, 1993, pp. 725–730.

[11] A. Piazzi, A. Visioli, Global minimum-time trajectory planning of mechanical manipulators using interval analysis, International Journal of Control 71 (4) (1998) 631–652.

[12] D. Constantinescu, E.A. Croft, Smooth and time optimal trajectory planning for industrial manipulators along specified paths, Journal of Robotic Systems 17 (2000) 233–249.

[13] M. Weck, A. Meylahn, C. Hardebusch, Innovative algorithms for spline-based CNC controller: production engineering research and development in Germany, Annals of the German Academic Society for Production Engineering VI/1 (1999) 83–86.

[14] Y. Altintas, K. Erkorkmaz, Feedrate optimization for spline interpolation in high speed machine tools, CIRP Annals 52 (2003) 297–302.

[15] R.V. Fleisig, A.D. Spence, Constant feed and reduced angular acceleration interpolation algorithm for multi-axis machining, CAD Computer Aided Design 33 (1) (2001) 1–15.

[16] T. Coleman, M.A. Branch, A. Grace, Optimization Toolbox for Use with MATLAB®, User's Guide Version 2, The MathWorks Inc., 1999.

[17] Y. Altintas, K. Erkorkmaz, W.-H. Zhu, Sliding mode controller design for high speed drive, Annals of CIRP 49 (1) (2000) 265–270.